IMPROVING DISTRIBUTION OF CRASH ENERGY ABSORPTION FOR CIVIL AIRCRAFT BASED ON PROGRESSIVE BENDING FAILURE MECHANISM

Tianjian Jiang[1], Zhangping Luo[1], Zi Kan[1], Jinwu Xiang[1], Xiaochuan Liu[2], Chunyu Bai[2] & Xulong Xi[2]

[1]School of Aeronautic Science and Engineering, Beihang University, Beijing, 100191, PR China
[2]Aircraft Strength Research Institute, Xi'an, PR China

Abstract

High level of civil aircraft crashworthiness is desired to provide as much protection as possible for occupant during a possible crash accident. This suggests the requirement inherent for assigning the energy absorption distribution in a fuselage structure according to design intention. Numerous works show that noticeable energy altering of component for conventional fuselage layout usually accompanies with unacceptable mass penalty and cost. In addition, it still remains significant difficulty to fulfill intended fuselage deformation mode. In this paper, the progressive bending failure mechanism of frame is employed to develop a crashworthy structure layout below the cabin floor. An appropriately constrained frame could be failure in a progressive manner under a transverse impact with moving contact surface, and then develops new deformation mode. Three energy absorption zones are formed naturally in the lower fuselage shell. The aim of the preliminary design study is to evaluate the crashworthiness aspects on fuselage section level. Finite element simulations for a two-frame fuselage section were performed at the vertical impact velocity of 7 m/s, and parameter analysis as well as comparison with a conventional counterpart were conducted. It was found that the level of energy absorption of the conventional fuselage is "high-mid-high" from the bottom zone to the top one, corresponding to the energy absorption percentages 35.0%, 25.3%, and 34.8%; whereas the presented fuselage is "mid-high-low", corresponding to 11.5%-37.3%, 44.2%-63.1%, and 6.0%-10.5%. At two occupant-seats position, the peak acceleration values are reduced by 12.5%-45.7%, and 16.4%-58.0%, respectively, with one exceptional increasing by 0.4% of the former. For all parameters, only one yields W-type deformation in the lower fuselage, the others are U-type.

Keywords: Civil Aircraft, Crashworthiness, Energy Absorption, Bending Failure

1. Introduction

Due to requirements for safety and economy, developing civil aircrafts demands for crashworthiness technology to reduce the cabin acceleration levels while fuselage structures provide appropriate crash energy absorption with restricted structure mass and cost. However, most of current technologies for possible crashworthy fuselage design often suffer significant mass penalty in providing stiff support structures for the cabin floor support struts or energy-absorbing devices in sub-cargo zone [1]. This leads to great difficulty to assign crash impact energy to specific structural components according to the design intention.

On the aspect of energy absorption distribution, experiments [2-4] indicate that structures under the cabin floor absorb most of the impact energy in a typical fuselage section. Usually, about 50% of impact energy is absorbed by the frames and remaining by the skin, struts, and supports under the cargo floor [5,6], and therefore the frames is regarded as the major role for the impact energy absorption. To improve crashworthiness of aircraft structure, much research work has been performed on the fuselage component altering, development of energy absorption devices [7], crash fuselage concept, and so on. Perez et al. [8] resized flanges of semicircular frames with I-section and showed the augmented energy absorption relative to original frames with static test results from both of these. While frames predominate in energy absorption, research on struts and structures

under cargo floor also attracts much attention. In [9] a composite crash absorber element was developed, absorbing energy by cutting the composite strut into stripes and crushing the material under bending. In [10] closed thin-walled composite tubes are investigated on the influence of section shapes and assembly details on energy absorption ability under dynamic and quasi-static crush test. Paz et al. [11-13] developed a kind of hybrid energy absorber and its applications to substitute the strut for improving crashworthiness of aircraft were investigated. Caprio et al. [14] designed a kind of composite stanchion for the cargo sub-floor structure of a civil aircraft, and the crash response of the support system under the cargo cross beam was also be investigated [15]. Waved beam is considered as a good load-carrying component and a good energy absorber. Installing such a structure under either cabin floor as longitudinal oblique beams [16], or sub-cargo zone as in-plane plate of cargo cross beam [17,18], were evaluated for augmenting energy absorption and reducing peak acceleration. A crushable subfloor structure concept was developed by segmentally introducing foam blocks between the cargo floor and the belly skin [19], and the analysis showed the high efficiency of energy absorption and remarkable effect in mitigating high peak acceleration value. Saiaf et al. [20] employ a PVC foam to fill in the space between the bottom of auxiliary fuel tank and the aluminum cargo floor to augment the crashworthiness of a newly developed civil aircraft, and outcomes from numerical simulation reveal that mitigation of maximum peak acceleration response can be 6% to 36%. Recently, a systematical development of crash concepts for composite transport aircraft is summarized in [1]. For the bend frame crash concept, 30% of the impact kinetic energy are assigned to the sub cargo structure. The outcomes indicate that the bend frame concept developed with progressive crushing of the sub-cargo structure, leads to the significant mass penalty for both of the cargo cross beam and the frame. This work highlights that the energy assignment is feasible, however limited by the significant need for structural stiffness, and consequently leads to opposite structural design feature [21].

In this paper, a crashworthy structure layout below the cabin floor is developed based on the progressive bending failure mechanism of frame. Generally, progressive failure is achieved by axially compressing an open section rod or closed section tube. A frame is a typical curved beam carrying moment and experiences transverse impact loads under crash scenario. For a metallic frame, plastic hinge and fracture are the usual failure modes. A global constraint to the frame and appropriate sub-cargo structure layout are found to promote a progressive bending failure behavior of frame under a transverse impact. Here focus on the characteristics of crash impact energy distribution, acceleration response, and deformation mode of the fuselage.

2. Fuselage Structural Layout

2.1 Principle

A drop test of structure under cabin floor of a fuselage section was conducted. Figure 1 show the state of a plastic hinge recorded by a high-speed camera. It could be found that the plastic hinge moves along the frame and stop at the position in vicinity of the cabin floor support strut attachment, see Figure 1(a) and Figure 1(b), indicated by circles, arrow indicating the initial position. Observing the deformation of the frame at the final state find a continuous slope exists between positions of the final plastic hinge and the frame center. So, it is a travelling hinge.

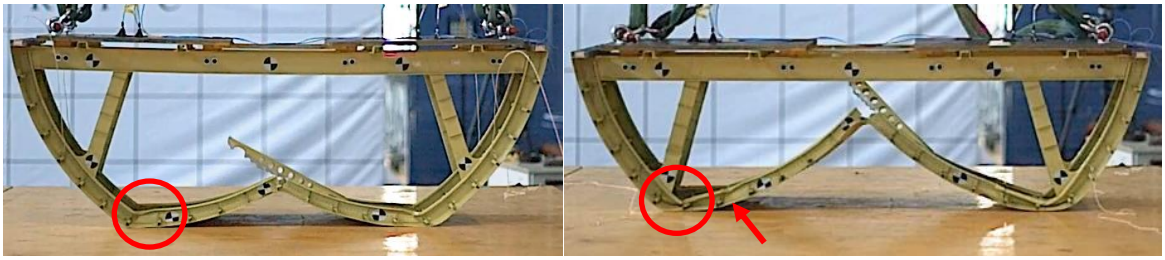

(a) (b)

Figure 1 – States of plastic hinge.

From the observation we can set constraints on the frame, as illustrated in Figure 2. Moving of a plastic hinge will be confined by neighboring constraints. Far end of the frame will be loaded further under the circumstance, and new plastic hinge would occurred. The process repeats till the kinetic

energy exhausts. The failure behavior could be called the progressive bending failure.

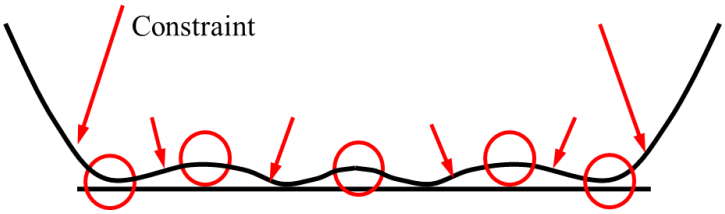

Figure 2 – Schematic of progressive bending failure.

2.2 Fuselage structural layout with progressive bending failure

The fuselage structural layout is developed based on a conventional single-aisle civil aircraft, which is similar to the one used in the previous experimental study [22]. As shown in Figure 3(b), main components under the cabin floor include cabin floor support strut, upper tilt rod, lower tilt rod, column, cargo beam, and frame. Columns under the cargo beam could easily change the stiffness level by changing the column thickness. Basic geometry dimensions of the fuselage are annotated in Figure 3(a), which is a conventional layout, used as the counterpart to compare with the presented fuselage structural layout.

Columns, tilt rods, struts, and cargo floor beam form a global constraint to the lower frame, and they are the crucial factors that altering the crashworthy behaviors of the fuselage.

For the presented layout, thickness of cabin floor support strut, upper tilt rod, lower tilt rod, and column are all 1.8 mm. When perform the parameter analysis, the strut, lower tilt rod, and column are selected, and take the same values of 0.6 mm and 3.0 mm as the thickness bound for all the three components. When the thickness of one component changes, the rest of the two components keeps their thickness 1.8 mm unchanged.

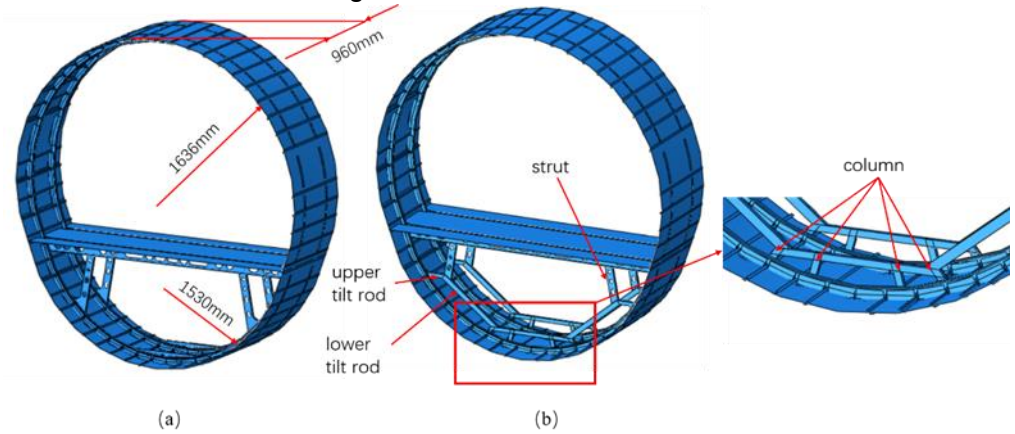

Figure 3 – Geometry of two fuselage sections: (a) conventional layout, (b) the presented layout

2.3 Energy absorption zone

Figure 4 gives three energy absorption zone according to the structure feature. The common boundaries of adjacent zones are divided into two halves from the middle to ensure no repeat count.

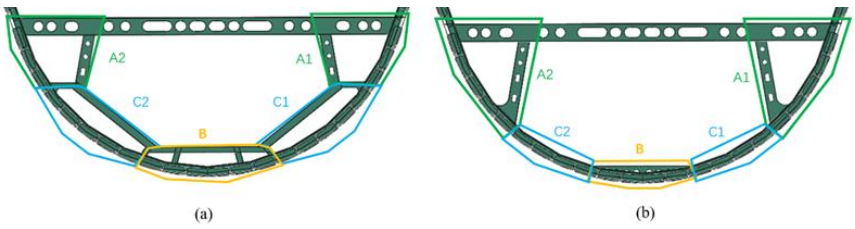

Figure 4 – Division of energy absorption zone: (a) presented layout, (b) conventional layout

During the impact, the energy absorption equation of the fuselage section is:

$$E_{TOT} = E_{KE} + E_I + E_{FR} - W \quad (1)$$

where E_{TOT} is the total energy, E_{KE} the kinetic energy, E_I the internal energy, E_{FR} the frictional dissipated energy, and W the external work of gravity. For the three zone A, B, and C, there is:

$$E_I = E_{IA} + E_{IB} + E_{IC} + E_{IOTHER} \quad (2)$$

where E_{IA}, E_{IB}, and E_{IC} are the internal energy of zone A, B, and C; E_{IOTHER} is the internal energy of structures other than the above three zones. In most crash accidents, E_{IOTHER} is quite low.

Obviously, compared to the conventional layout, more interaction exists between the adjacent zone in the presented layout because of their common boundaries. At the same time, the crushing load transmitting path between zone A and zone B is changed from the low stiffness frame to the high stiffness of zone C, which complicates the load transmitting path. In this way, the tilt rod and frame in zone C can deform and absorb impact energy simultaneously so that E_{IC} will be predominant with the decrease of E_{IA}.

To investigate whether the layout can realize our design goals, we use the finite element method to simulate impact accidents.

3. Finite Element Models

The finite element models are shown in Figure 5. The cabin beam, frame, strut, cargo cross beam, and sub-cargo panel are made of Al7075, while the cabin floor and skin are made of Al2024. The tilt rod and sub-cargo columns in the presented fuselage are made of Al7075. The properties of materials Al2024 and Al7075 are listed in table 1 and similar to those in [22]. The Johnson-Cook constitutive equation is used to simulate the damage and fracture of metal materials in the crash accident. A tie-contact relation is used to substitute the bolted connection. The impact velocity is 7.0 m/s, and the gravity acceleration is 9.8 m/s^2. Table 2 presents the mass of different fuselage section models. Table 3 shows the materials and thicknesses of different components in the conventional fuselage model. Mass of each occupant-seat block is 200 kg.

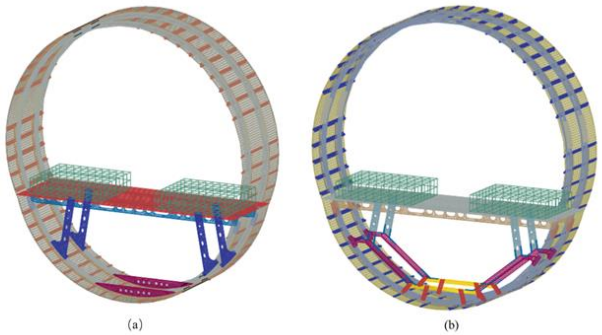

Figure 5 – Finite element models: (a) conventional layout, (b) presented layout

Table 1 Material properties of Al2024 and Al7075

material	Mass density/(kg·m^{-3})	Young's Modulus/(MPa)	Poisson's ratio	Yield stress/(MPa)	Ultimate failure/(%)
Al2024	2780	73100	0.33	324	9.5-14.6
Al7075	2810	71700	0.32	503	6.5-9.2

Table 2 Mass of different fuselage models

Fuselage model	Components	Thickness/(mm)	Model mass/(kg)
Presented	strut	0.6	184.614
		1.8	185.440
		3.0	186.268
	column	0.6	185.056
		1.8	185.440
		3.0	185.825
	lower tilt rod	0.6	184.382
		1.8	185.440
		3.0	186.499
Conventional			183.266

In our fuselage models, all components are modeled using shell elements due to their advantages and

convenience in thin-walled structures simulation. The thickness of these shell elements in different components is consistent with the corresponding components in the presented fuselage section. The impact deformation of conventional fuselage model and the test section in [22] has a good similarity. This means the finite element model in this paper can reflect the crash situation.

Table 3 Materials and thickness of different components in the conventional fuselage model

Component	Material	Thickness/(mm)
Strut	Al7075	1.8
Cabin floor	Al2024	11.0
Cabin beam	Al7075	3.2
Cargo cross beam	Al7075	1.8
Skin	Al2024	1.8

4. Results and Discussion

The conventional layout model and the presented layout models with different components thicknesses are simulated. The deformation, acceleration responses, and energy absorption of main components and different zones will be discussed. For a convenience description, in the following, the '0.6-strut' represents the presented layout model with the strut thickness of 0.6 mm, '3.0-column' means the presented fuselage model with column thickness of 3 mm, and '1.8-rod' means the presented fuselage model with the lower tilt rod thickness of 1.8 mm. Other similar expressions have the same meaning.

4.1 Fuselage Deformation

Figure 6 shows the maximum sub-cabin deformation and stress distribution diagram of the conventional fuselage and all presented fuselage models.

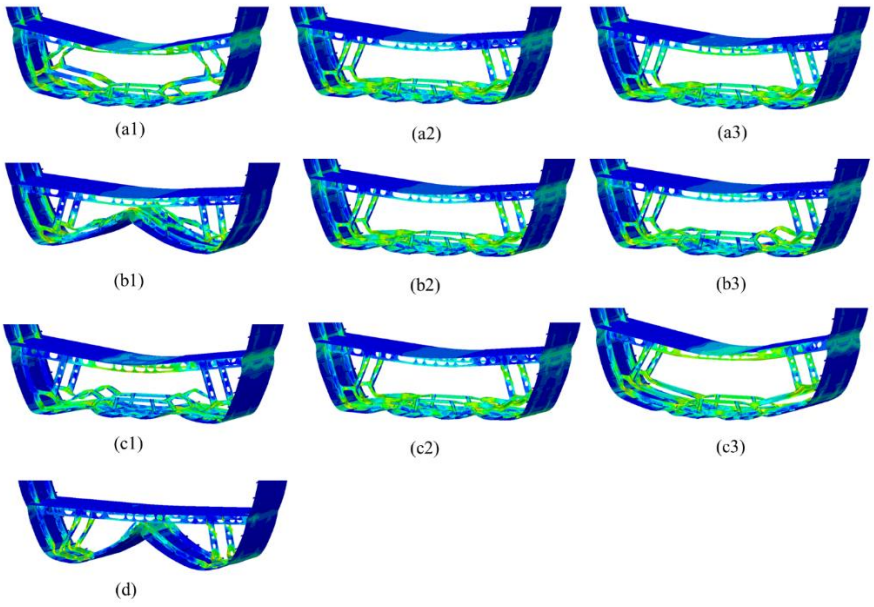

Figure 6 – Maximum sub-cabin deformation of all fuselage models: (a1) to (a3) energy absorption of the presented fuselage models from '0.6-strut' to '3-strut', (b1) to (b3) energy absorption of the presented fuselage models from '0.6-column' to '3-column', (c1) to (c3) energy absorption of the presented fuselage models from '0.6-rod' to '3-rod', (d) energy absorption of the conventional fuselage model

In the conventional fuselage, zone B contacts the cabin beam and zone C contacts the ground directly. This may lead to an unexpected impact on passengers in the cabin room, which has an adverse effect on crashworthiness. The struts bend and twist severely. Moreover, large deformation and destruction appear in zone B, struts and the junction of zones A and C. Compared to the conventional fuselage, the deformation is quite different. No contact between zone A and ground occurs. Expect the '0.6-column' fuselage, zone B in other presented fuselage models has slight deformation. Also, the tilt rod deformation significantly. In the presented fuselages, a lower element thickness leads to a more considerable deformation in this zone. In particular, a low thickness of the strut in zone B can result in a change of deformation mode: zone B bends inward and move upward. The deformation seems encouraged since they are U type and buckle the fuselage outward [23].

4.2 Acceleration Responses

Figures 7 and 8 present the acceleration responses of all fuselage models. In this paper, we additionally calculate the mean absolute acceleration. Table 4 shows the peak, mean acceleration, and mean absolute acceleration of different fuselage models. The acceleration response curve is from the center point of the upper face of the two passenger squares. Point 1 locates at the center point of the upper face of the left passenger square and point 2 locates at that of the right square. The a_{1max}, $\overline{a_1}$, and $\overline{|a_1|}$ represent the peak acceleration, mean acceleration and mean absolute acceleration of point 1, and a_{2max}, $\overline{a_2}$, and $\overline{|a_2|}$ for position 2. All acceleration data has been filtered using the Butterworth low-pass filter to eliminate high-frequency noise.

The peak acceleration of the conventional fuselage model is 25.6 g and 30.5 g which are higher than most of the presented fuselage sections. The minimum peak acceleration at point 1and point 2 of the presented fuselage models is 13.9 g and 12.8 g which both appear in the '0.6-column' model. Compared to the conventional fuselage, the reduction is 45.7 % and 58.0 %. The mean acceleration at point 1 of the presented fuselage is generally high than that of the conventional fuselage while some of the mean acceleration at point 2 is quite low. At point 1, only the '0.6-strut' fuselage has a lower mean acceleration than the conventional fuselage and the reduction is 19.3%. At point 2, the minimum mean acceleration is -0.4 g. This indicates that a high level of downward acceleration occurs. As for mean absolute acceleration, in most of the presented fuselage, they are lower. This indicates that the presented fuselage can reduce the peak and mean absolute acceleration effectively.

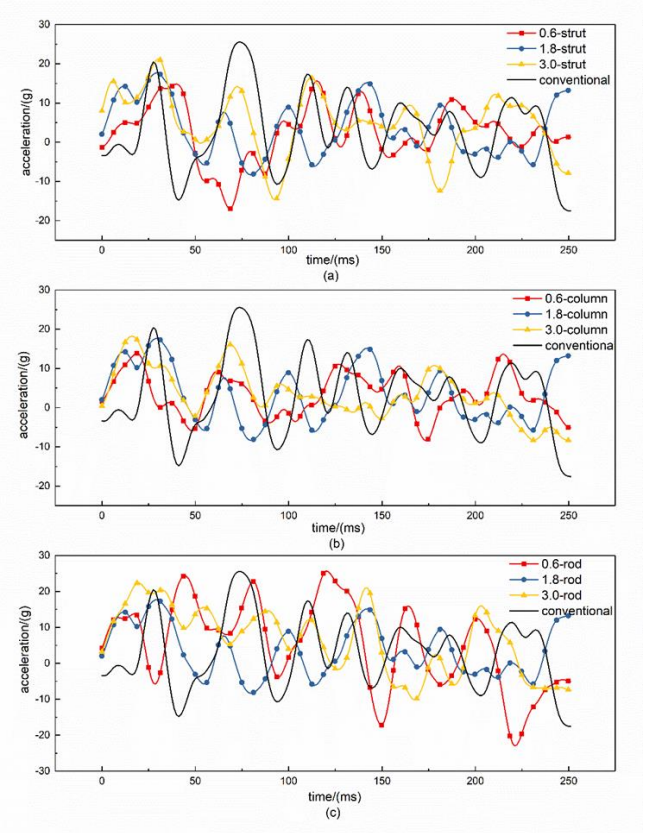

Figure 7 – Acceleration curves at point 1 of models of different component thickness. (a) strut, (b) column, (c) lower tilt rod

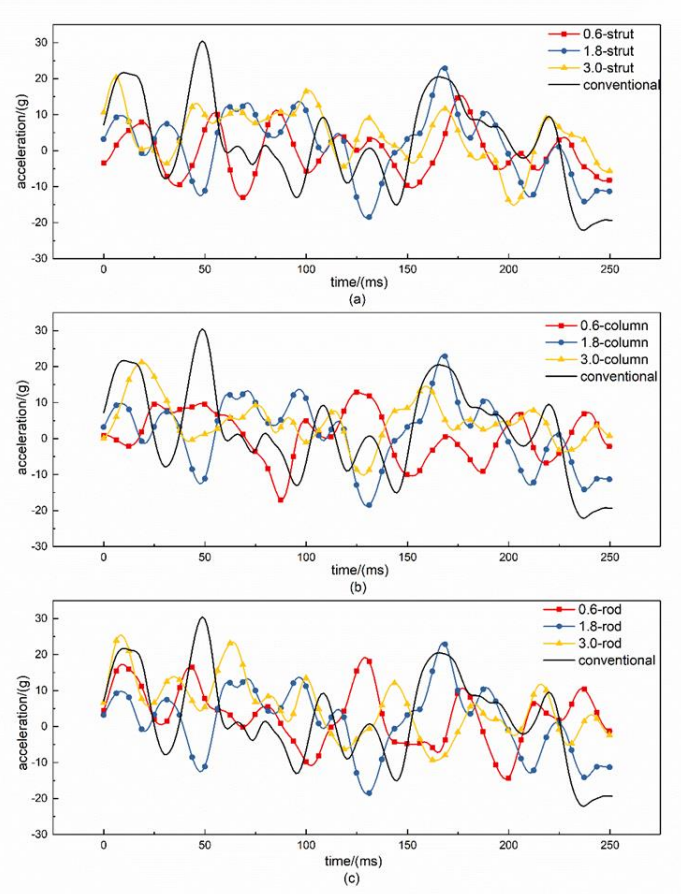

Figure 8 – Acceleration curves at point 2 of models of different component thickness. (a) strut, (b) column, (c) lower tilt rod

Table 4 Acceleration data of different fuselage models

	Fuselage model	a_{1max}/(g)	$\overline{a_1}$/(g)	$\overline{\lvert a_1 \rvert}$/(g)	a_{2max}/(g)	$\overline{a_2}$/(g)	$\overline{\lvert a_2 \rvert}$/(g)
Presented	0.6-strut	15.7	2.5	5.9	15.3	-0.4	5.3
	1.8-strut	17.7	3.6	6.2	23.2	1.5	7.8
	3.0-strut	21.2	4.9	7.9	20.4	4.3	6.9
	0.6-col	13.9	3.4	5.1	12.8	0.8	5.5
	1.8-col	17.7	3.6	6.2	23.2	1.5	7.8
	3.0-col	18.2	3.5	5.4	21.2	4.6	5.9
	0.6-rod	25.7	5.3	11.0	19.1	2.9	6.7
	1.8-rod	17.7	3.6	6.2	23.2	1.5	7.8
	3.0-rod	22.4	6.4	9.5	25.5	5.3	7.5
Conventional		25.6	3.1	8.1	30.5	2.5	9.8

The influence of the element thickness on acceleration response is also noticeable. We first make a comparison of different thicknesses of the strut. Obviously, the best acceleration response appears in the '0.6-strut' fuselage because low strut thickness reduces the load transmitting to the passengers. When the thickness is 3.0 mm, the peak, mean, and mean absolute acceleration are all higher. As for the middle thickness of 1.8 mm, the acceleration response of the two points is quite different but the mean acceleration is still lower than that of the fuselage of 3.0 mm thickness. From Figure 7 and 8, we can tell that these three acceleration curves at point 1 have an initial peak before 50 ms and their peak values duration increase with the increase in thickness. At point 2, the initial peak is less obvious when the thickness is 0.6 mm and 1.8 mm, but the change trend is the same. This derives

from the reduced load caused by the low thickness of the strut. In general, the results show that the low thickness of the strut can reduce the acceleration response of passengers.

As for the column, we should observe the acceleration responses of the '0.6-column', '3-column' and '1.8-column' models. The lowest acceleration response appears in the '0.6-column' fuselage case. This arises from the more deformation and energy absorption in zone B caused by the low thickness of the columns. When the column thickness is 3.0 mm, the acceleration response of the two points is both high but is not much different from the thickness of 1.8 mm. In general, the influence of the column thickness is similar to that of the strut thickness.

As for the thickness of the lower tilt rod, the influence is quite different. At point 1, when the thickness is 0.6 mm, the peak acceleration is 25.7 g, higher than that of the two other fuselages and the conventional fuselage. The mean and mean absolute acceleration are also higher. As for point 2, though the peak acceleration is relatively low, the mean acceleration is higher than that of the fuselage of 1.8 mm thickness case. The low thickness of the lower tilt rod cannot provide enough constraint for the strut thus the acceleration is low in the initial impact phase step and high in the middle and large steps. When the thickness of the lower tilt rod is 3.0 mm, the acceleration response is also terrible. Obviously, the high thickness of the lower tilt rod has more constraints for the strut and easily causes a high acceleration response. Therefore, the too low and too high thickness of the low tilt rod both have an adverse effect on the acceleration response of the passengers.

4.3 Energy absorption of component

Figure 9 presents the energy absorption results of the whole model, frame, strut, and tilt rod of the conventional fuselage model and all presented fuselage models. Here, the tilt rod is the sum of the upper and lower tilt rod. And table 5 shows the energy absorption results of these models at 250 ms. E_{Ifra}, E_{Irod}, and E_{Istr} are the energy absorption of the frame, tilt rod, and strut.

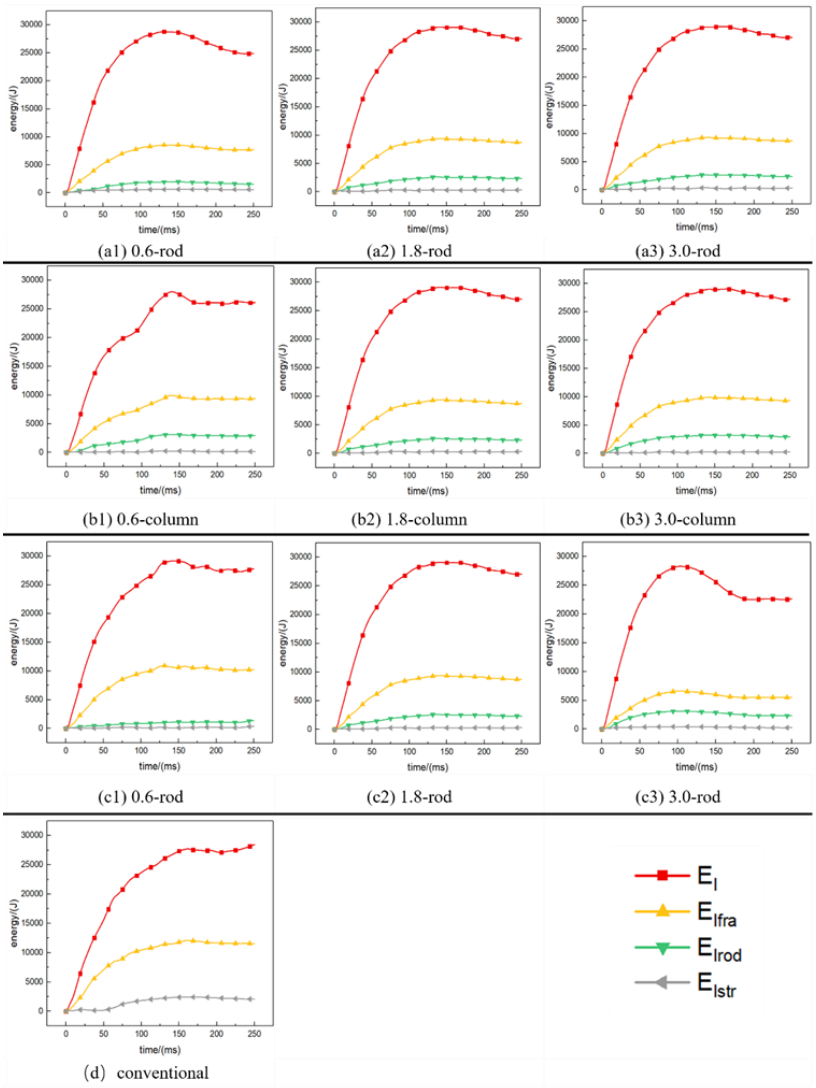

Figure 9 – Energy absorption of component of all fuselage models: (a1) to (a3) energy absorption of the presented fuselage models from '0.6-strut' to '3-strut', (b1) to (b3) energy absorption of the presented fuselage models from '0.6-column' to '3-column', (c1) to (c3) energy absorption of the presented fuselage models from '0.6-rod' to '3-rod', (d) energy absorption of the conventional fuselage model.

Table 5 Energy absorption of component

	Fuselage model	E_I/(J)	E_{Ifra}/(J)	E_{Irod}/(J)	E_{Istr}/(J)	$\frac{E_{Ifra}}{E_I}$	$\frac{E_{Irod}}{E_I}$	$\frac{E_{Istr}}{E_I}$
Presented	0.6-strut	24878	7687	1506	577	30.9%	6.1%	2.3%
	1.8-strut	27027	8723	2344	297	32.3%	8.7%	1.1%
	3-strut	27055	8680	2373	311	32.1%	8.8%	1.1%
	0.6-col	26127	9369	2924	153	35.9%	11.2%	0.6%
	1.8-col	27027	8723	2344	297	32.3%	8.7%	1.1%
	3.0-col	27203	9344	2943	255	34.3%	10.8%	0.9%
	0.6-rod	27777.	10218	1347	354	36.8%	4.8%	1.3%
	1.8-rod	27027	8723	2344	297	32.3%	8.7%	1.1%
	3.0-rod	22620	5489	2310	231	24.3%	10.2%	1.0%
Conventional		28454	11541		2064	40.6%		7.3%

We can find that the existence of the tilt rod reduces E_{Ifra} effectively. In the conventional fuselage model, E_{Ifra} is 11541 J and 40.6% of E_I, while in the presented fuselage models, the minimum value is 5489 J and 24.3%, appearing in the '3.0-rod' fuselage model. The highest E_{Irod} is 2943 J in the '3.0-column' fuselage and the highest percentage is 11.2% in the '0.6-column' fuselage. Meanwhile, compared to the conventional fuselage, the energy absorption of the strut in presented fuselage models decreases significantly. In the conventional fuselage model, E_{Istr} is 2064 J and 7.3% of E_I, while the maximum value of them is 577 J and 2.3% in the presented fuselage models.

The thickness of elements in different zones also has different influences on element energy absorption distribution. As for E_I, a high level of the strut thickness means more energy absorption while it is opposite for the lower tilt rod. The influence of element thickness on E_I is most significant when the thickness of the lower tilt rod changes, which drops from 27777 J in the '0.6-rod' fuselage to 22620 J in the '3-rod'. This indicates that changing the thickness of the lower tilt rod can effectively control the energy absorption of the whole model. Unlike the conventional fuselage, all presented fuselage models exist a rebound phenomenon at the final phase, especially in '0.6-strut and '3-column' fuselage cases.

The thickness of the strut and column has little effect on E_{Ifra}. The difference between the maximum and minimum of E_{Ifra} is 993 J and 646 J in the three strut and column thicknesses, while it is 4729 J in the three lower tilt rod thicknesses. In general, the thickness of the lower tilt rod dominates the E_{Ifra} and a higher thickness leads to a smaller energy absorption.

As for the tilt rod, energy absorption increases from 4.8% to 11.2% as the thickness of the strut and lower tilt rod increases. And the latter has greater influence, accounting for 4.8% in '0.6-rod' fuselage and 10.2% in '3.0-rod' fuselage. As for the column thickness, the percentage is lowest when the thickness is 1.8 mm.

4.4 Zone Energy Absorption

Table 6 shows the energy absorption of three zones in different models at 250 ms.

In the conventional fuselage model, the energy absorption of the three zones is very close. The $\mathrm{E_{IA}}$, $\mathrm{E_{IB}}$, and $\mathrm{E_{IC}}$ account for 34.8%, 35.0%, and 25.3% of the $\mathrm{E_I}$. In the presented fuselage models, the energy distribution of the three zones is quite different. The energy absorption percentage of zone A decreases significantly. And the maximum and minimum percentages of $\mathrm{E_{IA}}$ are 10.5% and 6.0%, which appear in '0.6-strut' and '3.0-column' fuselage. Except for the '0.6-column' fuselage, the percentage of $\mathrm{E_{IB}}$ also decreases and the minimum is 11.5%, which appears in the '0.6-strut'

fuselage. As for zone C, the percentage of E_{IC} increases, and the maximum is 63.1% in '0.6-rod' fuselage. This indicates that the presented fuselage design can concentrate the impact energy to zone C and reduce the energy absorbed by zones A and B.

The element thickness also influences zone energy absorption. First, we discuss the thickness of the strut in zone A. When strut thickness is 0.6 mm, the E_{IA} is highest while the situation of E_{IB} and E_{IC} are opposite. Meanwhile, when the thickness is 1.8 mm and 3.0 mm, the zone energy absorption distribution has little difference. The reason is as follows: zone A has the highest position in the sub-cabin structure and the impact load is transmitted from bottom to top. Thus, when the strut stiffness level decreases, the energy absorbing ability of zone A reduces and the other two zones absorb more impact energy. Meanwhile, when the stiffness level of the strut is low, the zone energy distribution is more sensitive to the changing of stiffness.

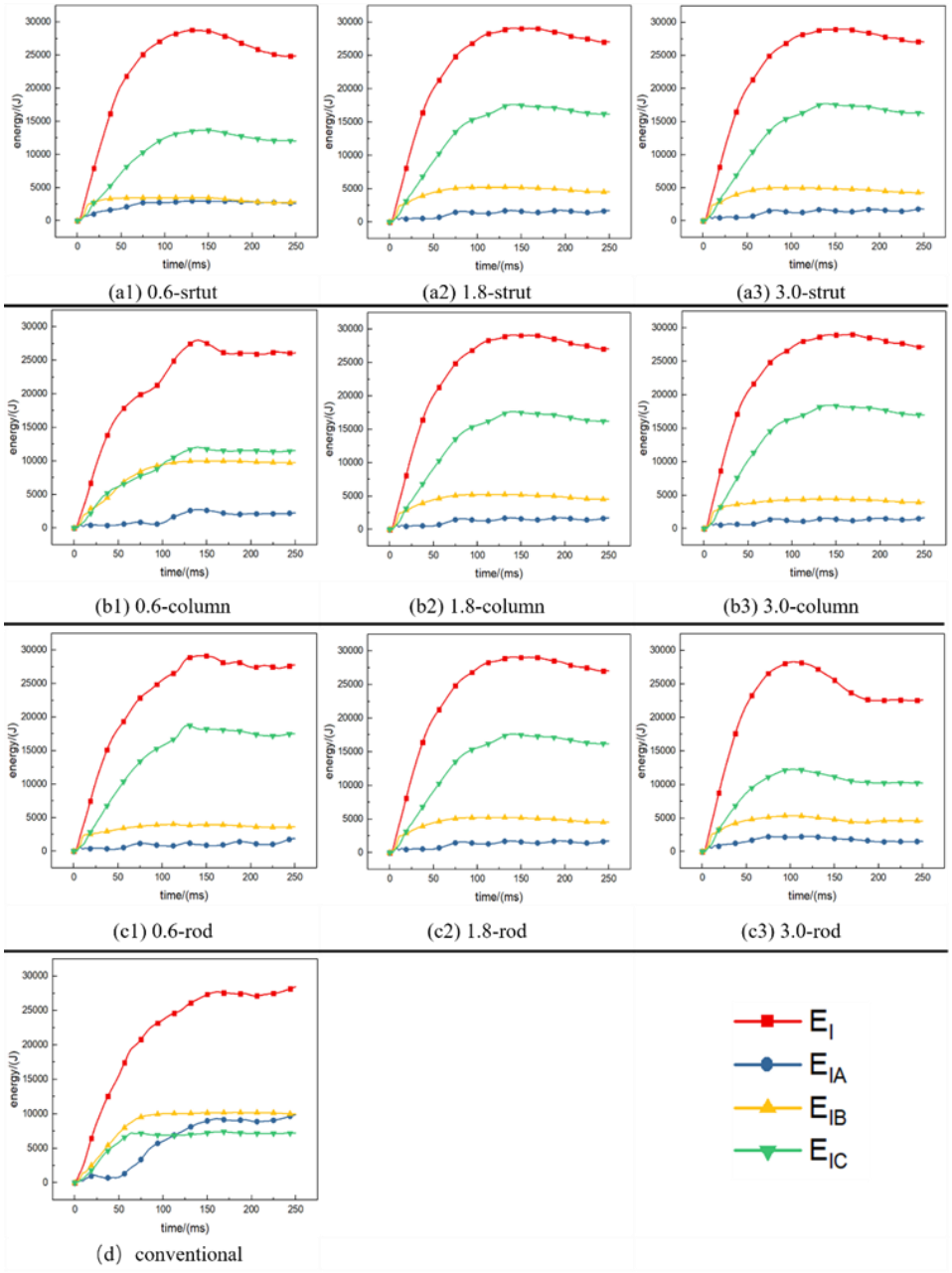

Figure 10 – Energy absorption of zone: (a1) to (a3) energy absorption of the presented fuselage models from '0.6-strut' to '3-strut', (b1) to (b3) energy absorption of the presented fuselage models from '0.6-column' to '3-column', (c1) to (c3) energy absorption of the presented fuselage models from '0.6-rod' to '3-rod', (d) energy absorption of the conventional fuselage model

Table 6 Energy absorption of zone

	Fuselage model	E_I/(J)	E_{IA}/(J)	E_{IB}/(J)	E_{IC}/(J)	$\frac{E_{IA}}{E_I}$	$\frac{E_{IB}}{E_I}$	$\frac{E_{IC}}{E_I}$
Presented	0.6-strut	24878	2606	2871	12047	10.5%	11.5%	48.4%
	1.8-strut	27027	1722	4520	16213	6.4%	16.7%	60.0%
	3.0-strut	27055	1792	4261	16281	6.6%	15.7%	60.2%
	0.6-col	26127	2241	9734	11542	8.6%	37.3%	44.2%
	1.8- col	27027	1722	4520	16213	6.4%	16.7%	60.0%
	3.0-col	27203	1619	3918	16987	6.0%	14.4%	62.4%
	0.6-rod	27777	1880	3615	17514	6.8%	13.0%	63.1%
	1.8-rod	27027	1722	4520	16213	6.4%	16.7%	60.0%
	3.0-rod	22620	1512	4546	10214	6.7%	20.1%	45.2%
Conventional		28454	9890	9964	7195	34.8%	35.0%	25.3%

As for the thickness level of the sub-cargo column, the $\mathrm{E_{IA}}$ and $\mathrm{E_{IB}}$ decrease when it increases and the $\mathrm{E_{IC}}$ is opposite. In the '0.6-column' fuselage, the $\mathrm{E_{IB}}$ and $\mathrm{E_{IC}}$ have little difference and they are nearly five times of $\mathrm{E_{IA}}$. Meanwhile, the percentage of $\mathrm{E_{IB}}$ is highest in all presented fuselages. Zone B locates at the bottom of the sub-cabin structure. When its thickness is 1.8 mm and 3.0 mm, $\mathrm{E_{IB}}$ decreases and only counts for one-fifth of $\mathrm{E_{IC}}$. This indicates that the energy absorption of zone B can be effectively controlled by changing the column thickness.

When the thickness of the lower tilt rod increases, the percentage of $\mathrm{E_{IB}}$ increases while that of $\mathrm{E_{IC}}$ is opposite. the percentage of $\mathrm{E_{IC}}$ is 63.1% in '0.6-rod' fuselage which is highest in all presented fuselages. The percentage of $\mathrm{E_{IA}}$ nearly remains unchanged. Zone C is in the middle of the sub-cabin structure and plays a key role in connecting top and bottom structures in sub-cabin space. Thus, if the stiffness of the lower tilt rod is low, the energy absorbing distribution will show polarization and more energy will be absorbed by this zone. The energy absorbing distribution will be relatively even when the stiffness level is high, just as the '3.0-rod' fuselage model.

5. Conclusion

The purpose of this paper is to provide an aircraft crashworthy design method via changing energy absorption distribution mechanisms. Based on progressive bending failure, the method aims to change and control the percentage of the energy absorption of different zones as expected. The finite element method is used to investigate how the layout can realize the change and control of the expected energy absorption distribution and the crashworthiness can be improved. The results are as follows:

(1) Below the cabin floor, the energy absorption from bottom to top changes from the distribution of 'high-mid-high' in the conventional fuselage to the distribution of 'mid-high-low' in the presented fuselage, and the energy absorption of the frame and acceleration response of the occupants can also be decreased.

(2) Changing the thickness of the strut, column, and the lower tilt rod, the energy absorption distribution can be effectively controlled.

(3) Except for the thickness of the low tilt rod, acceleration will be lower when the other two element thickness decreases.

6. Contact Author Email Address

luozp@buaa.edu.cn

7. Copyright Statement

References

[1] Waimer M, Feser T, Schatrow P and Schueler D. Crash concepts for CFRP transport aircraft – comparison of the traditional bend frame concept versus the developments in a tension absorbers concept. *International journal of crashworthiness*, Vol. 23, No. 2, pp 193-218, 2018.

[2] Williams M S and Hayduk R J. Vertical drop test of a transport fuselage section located forward of the wing. *NASA Technical Memorandum M.85679*, 1983

[3] Liu X, Sun X, Guo J and Mou R. Crash simulation and drop test of civil airplane fuselage section. *Proceedings 2013 International Conference on Mechatronic Sciences, Electric Engineering and Computer*, Shenyang, 2013.

[4] Zhang X, Xi X, Liu X and Bai C. Experimental study on crash characteristics of typical metal civil aircraft fuselage structure. *ACTA AERONAUTICAET ASTRONAUTICA SINICA*, Vol. 43, No. 6, pp 526234-1-526234-14, 2022

[5] Byar A. *Crashworthiness study of a Boeing 737 fuselage section (A)*. Drexel University, 2004

[6] Xue P, Ding M, Qiao C and Yu T. Crashworthiness study of a civil aircraft fuselage section. *Latin American Journal of Solids and Structures*, Vol. 11, No. 9, pp 1615-1627, 2014.

[7] Mou H, Xie J and Feng Z. Research status and future development of crashworthiness of civil aircraft fuselage structures: An overview. *Progress in Aerospace Sciences*, Vol. 119, 2020

[8] Perez J G, Johnson E R and Boitnott R L. Design and test of semicircular composite frames optimized for crashworthiness. *39th AIAA/ASME/ASCE/AHS/ASC Structures, Structural Dynamics, and Materials Conference and Exhibit*, Long Beach, CA, AIAA-98-1703, pp 27-38, 1998.

[9] Heimbs S, Strobl F, Middendorf P and Guimard J M. Composite crash absorber for aircraft fuselage applications. *WIT Transactions on the built environment,* Vol. 113, pp 3-14, 2010.

[10] Jackson A, David M, Gunnion A J, Kelly D and Dutton S. Dynamic and quasi-static crush testing of closed carbon-fibre/epoxy elements. *Proc of the 27th Congress of International Council of the Aeronautical Sciences*, Nice, France, ICAS 2010-9.8.1, pp 1-9, 2010.

[11] Paz J, Díaz J and Romera L. Crashworthiness analysis and enhancement of aircraft structures under vertical impact scenarios. *Journal of Aircraft*, Vol. 57, No. 1, pp 3-12, 2020.

[12] Paz J, Romera L and Díaz J. Crashworthiness optimization of aircraft hybrid energy absorbers enclosing honeycomb and foam structures. *AIAA Journal*, Vol. 55, No. 2, pp 652-661, 2017.

[13] Paz J, Díaz J, Mendez J, Romera L and Teixeira-Dias F. Crashworthiness study on hybrid energy absorbers as vertical struts in civil aircraft fuselage designs. *International journal of crashworthiness*, Vol. 25, No. 4, pp 430-446, 2020.

[14] Caprio D F, Ignarra M, Marulo F, Guida M, Lamboglia A and Gambino B. Design of composite stanchions for the cargo subfloor structure of a civil aircraft. *Procedia engineering*, Vol. 167, pp 88-96, 2016

[15] Riccio A, Saputoa S, Sellittoa A and Caprio D F. On the crashworthiness behaviour of a composite fuselage Sub-floor component. *Composite Structures*, Vol. 234, 2020.

[16] Wiggenraad J F M, Santoro D, Lepage F, Kindervater C and Climent Manez H. Development of a crashworthy composite fuselage concept for a commuter aircraft. *NLR Report NLR-TP-2001-108*, 2001.

[17] Zheng J, Xiang J, Luo Z and Ren Y. Crashworthiness layout of civil aircraft using waved-plate for energy absorption. *ACTA AERONAUTICAET ASTRONAUTICA SINICA*, Vol. 31, No. 7, pp 1396-1402, 2010.

[18] Ren Y, Xiang J, Zheng J and Luo Z. Crashworthiness analysis of aircraft fuselage with sine-wave beam structure. *Chinese Journal of Aeronautics*, Vol. 29, No. 2, pp 403-410, 2016.

[19] Zheng J, Xiang J, Luo Z and Ren Y. Crashworthiness design of transport aircraft subfloor using polymer foams. *International Journal of Crashworthiness*, Vol. 16, No. 4, pp 375-383, 2011.

[20] Saiaf B R, Xue P. Crashworthiness Study of a newly developed civil aircraft fuselage section with auxiliary fuel tank reinforced with composite foam. Aerospace, Vol. 10, No. 314, pp 1-14, 2023.

[21] Guida M, Lamanna G, Marulo F and Caputo F. Review on the design of an aircraft crashworthy passenger seat. *Progress in Aerospace Sciences*, Vol. 129, 2022.

[22] Liu X, Guo J, Sun X and Mu R. Drop test and structure crashworthiness evaluation of civil airplane fuselage section with cabin interiors. *ACTA AERONAUTICAET ASTRONAUTICA SINICA*, Vol. 34, No. 9, pp 2130-2140, 2013.

[23] Zimmermann R E and Merritt N A. Aircraft crash survival design guide, Vol. 1. *USAAVSCOM TR 89-D-22A*, Simula Inc, 1989.